

Expression of the VEGF-Related Factor Gene in Pre- and Postnatal Mouse

Jacob Lagercrantz,^{*,1} Catharina Larsson,^{*} Sean Grimmond,[†] Magnus Fredriksson,[‡]
Günther Weber,^{*} and Fredrik Piehl[§]

^{}Department of Molecular Medicine, L6 building, Karolinska Hospital, S-171 76 Stockholm, Sweden; [§]Department of Neuroscience, Karolinska Institute, S-171 77 Stockholm, Sweden; [†]Queensland Cancer Fund Research Unit, Joint Experimental Oncology Program, Queensland Institute of Medical Research, Herston, QLD, 4029, Australia; and [‡]The Wenner-Gren Institute, The Arrhenius Laboratories F3, Stockholm University, S-106 91 Stockholm, Sweden*

Received January 16, 1996

We have previously identified a novel gene closely related to the vasoactive endothelial growth factor (VEGF) gene. The human VEGF related factor (VRF) gene was initially isolated using an 11q13 specific cosmid probe (D11S750). Subsequently human VRF was used to isolate the corresponding mouse gene (*vrf*). Here, we report the spatiotemporal expression pattern of *vrf* during pre- and postnatal mouse development. Mouse *vrf* gene expression starts early in fetal development. At day 14 post coitum it is expressed in most cells of the embryo although the heart, spinal cord and the cerebral cortex show significantly higher levels of expression than other tissues. At 17 days post coitum expression is almost exclusively seen in heart, brown fat and spinal cord. This pattern of expression could be consistent with a role of *vrf* as a growth factor in these tissues. © 1996 Academic

Press, Inc.

Vasoactive endothelial growth factor (VEGF), also known as vasoactive permeability factor (VPF) is a secreted, covalently linked homodimeric glycoprotein that specifically activates endothelial tissues (1–3). This factor is involved in a variety of physiological processes including normal angiogenesis and a diversity of pathological processes characterized by rapid vessel formation (3).

When isolating genes from the q13 region on human chromosome 11 (4), a set of previously undescribed genes were identified (5–7). The product of one of these cDNAs (Grimmond et al., submitted) (GenBank accession number U43368 and U43369) was designated VRF (VEGF Related Factor), due to striking sequence homology to VEGF. The mouse gene (*vrf*) was subsequently isolated (Townson et al., submitted) (GenBank accession number U43836 and U43837) and found to have a very similar genomic organization to the human gene. The products of the human and mouse genes share 86% identity and 92% conservation of amino acid residues over the entire coding region.

Both human VRF and mouse *vrf* mRNAs are alternately spliced to produce at least two messages with open reading frames of 621 and 564 bp respectively and the predicted translation of these two isoforms gives rise to proteins with different carboxyl ends due to a shift in the open reading frame. Both protein isoforms show strong homology to VEGF at their amino termini but only the product of the shorter of the two mRNAs maintains homology to VEGF at its carboxyl terminus. In the VEGF165 and VEGF189 isoforms there are 16 cysteine residues, many of which aid in the dimerisation of these molecules (8), and which are conserved in position in the shorter of the VRF isoforms.

To shed light on the possible role of *vrf* as a growth factor during development we have

¹ To whom correspondence should be addressed. Fax: +46 8 327734.

Abbreviations: VEGF, Vasoactive endothelial growth factor; VPF, vasoactive permeability factor; VRF, VEGF Related Factor; nt, nucleotide.

investigated its expression pattern in embryonic and postnatal mice with *in situ* RNA hybridization histochemistry.

MATERIALS AND METHODS

Animals. Timed pregnant (n=4) and young adult (n=2) mice (C57 inbred strain, ALAB, Sweden) were sacrificed with carbon dioxide, and the relevant tissues were taken out and frozen on a chuck. Tissues were kept at -70°C until further use. Three gestational ages were used in this study; embryonic day 8 (E8), E14, and E17. All animal experiments in this study were approved by the local ethics committee for animal experimentation.

Northern blots. Mice were exposed to 4°C for varying periods of time to stimulate growth of brown fat tissues, as described earlier (9). Northern blots of total RNA from these brown fat tissues were generated in a manner similar to what has been described earlier (10).

In situ hybridization histochemistry. *In situ* hybridization was performed as previously described (11). Briefly, transverse sections ($14\mu\text{m}$) were cut in a cryostat (Microm, Germany), thawed onto Probe-On slides (Fisher Scientific, USA) and stored in black sealed boxes at -70°C until used. The sequences of the synthetic 42-mer oligonucleotides complementary to mRNA encoding *vrf* were ACCACCACCT CCCTGGGCTG GCATGTGGCA CGTGCATAAA CG (complementary to nt 120–161) and AGTTGTTTGA CCACATTGCC CATGAGTCC ATGCTCAGAG GC (complementary to nt 162–203). To detect the two alternative splice forms oligonucleotides GATCCTGGGG CTGGAGTGGG ATGGATGATG TCAGC-TGG (complementary to nt 484–521) and GCGGGCAGAG GATCCTGGGG CTGCTGGCCT CACAGCACT (complementary to nt 391–407 and 509–531) were used. The probes were labeled at the 3'-end with deoxyadenosine-alpha [thio]triphosphate [^{35}S] (NEN, USA) using terminal deoxynucleotidyl transferase (IBI, USA) to a specific activity of $7\text{--}10 \times 10^8$ cpm/ μg and hybridized to the sections without pretreatment for 16–18 h at 42°C . The hybridization-mixture contained: 50% formamide, $4 \times \text{SSC}$ ($1 \times \text{SSC} = 0.15\text{M NaCl}$ and 0.015M sodium-citrate), $1 \times$ Denhardt's solution (0.02% each of polyvinyl-pyrrolidone, BSA and Ficoll), 1% sarcosyl (N-lauroylsarcosine; Sigma), 0.02M phosphate buffer (pH 7.0), 10% dextran sulfate (Pharmacia, Sweden), 250 $\mu\text{g}/\text{ml}$ yeast tRNA (Sigma), 500 $\mu\text{g}/\text{ml}$ sheared and heat denatured salmon sperm DNA (Sigma) and 200mM dithiothreitol (DTT; LKB, Sweden). In control sections, the specificity of both probes was checked by adding a 20-fold excess of unlabeled probe to the hybridization mixture. In addition adjacent sections were hybridized with a probe unrelated to this study which gave a different expression pattern. Following hybridization the sections were washed several times in $1 \times \text{SSC}$ at 55°C , dehydrated in ethanol and dipped in NTB2 nuclear track emulsion (Kodak, USA) and overlaid with cover-slips. In some cases, sections were exposed to autoradiographic film (Beta-max autoradiography film Amersham Ltd, UK) prior to emulsion-dipping.

RESULTS

All four *vrf* oligonucleotide probes gave identical hybridization patterns in every tissue examined. Mouse *vrf* expression was detected in the 8 day old embryos (E8), in which positive signals were recorded over structures most likely corresponding to the neuronal tube (not shown). In sagittal sections of E14 mouse embryos the strongest hybridization signal was present over heart and in the nervous system, especially the cerebral cortex (fig. 1A). A low level of expression was present in some other tissues investigated. At a later gestational age, E17, a high *vrf* mRNA signal was confined to the heart and brown fat tissue in the interscapular region and around the neck (fig. 1B). Clearly positive hybridization signals were present in the gray of the spinal cord and in the tongue (fig. 1B). Expression in the cerebral cortex was clearly reduced compared to day 14. The weak background expression seen in the E14 embryo, in for example muscle, had decreased at this gestational age. A strong *vrf* mRNA hybridization signal was present solely over the heart and in the brown fat in young adult mice (fig. 1C). The signal over the heart was evenly distributed over the entire ventricular wall, including the papillary muscles (fig. 1D). In sections of heart tissue hybridized with an excess of cold probe, no specific labeling over background signal was recorded (fig. 1E).

Apart from the heart, *vrf* mRNA signal was present over certain tissues on the outside of the thoracic cage that morphologically resembled brown fat. That this indeed corresponded to fat tissues was verified with Sudan black counterstaining, which showed strong staining in the same areas (fig. 2A and 2B). The four *vrf* oligonucleotide probes, were hybridized to Northern blots of murine brown fat tissue total RNA and all showed an intense signal of the expected size (results

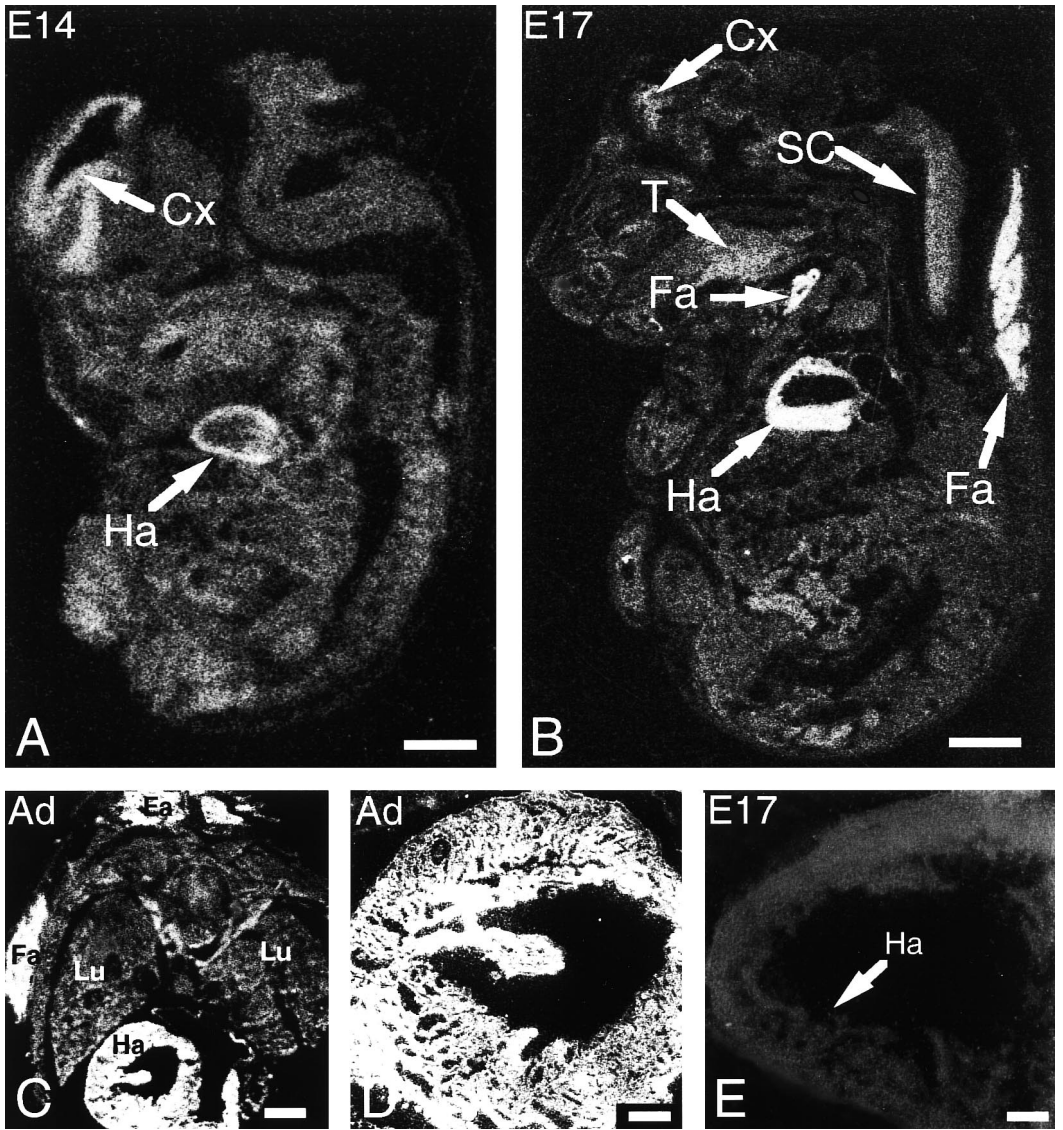


FIG. 1. Film autoradiographs (A–C) and dark-field micrographs (D–E) illustrating the expression pattern of *vrf* mRNA in the mouse. In the E14 mouse embryo (A) positive signals are present over the developing heart (Ha) and cerebral cortex (Cx). A low background signal is also present over other tissues in the section. In the E17 embryo (B) the heart (Ha) is clearly visible due to a strong hybridization signal. An equally strong signal is present over brown adipose tissue (Fa) in the back and around the thoracic cage. A moderate hybridization signal is present over the spinal cord (SC), the tongue (T) and the cerebral cortex (Cx). The background signal is reduced compared with the E14 embryo. In the young adult mouse (C–D), positive signals are present over the heart (Ha) and adipose tissue (Fa) around the thoracic cage, while, for example, the lungs (Lu) are unlabeled. The hybridization signal over the heart is evenly distributed over the entire left ventricle, including papillary muscles (D). In the E17 heart hybridized with an excess of cold probe, no positive signal is present (E). Scale bars: 0.5 mm (A), 1.2 mm (B), 1 mm (C), 0.3 mm (D), 0.1 mm (E).

not shown), thus verifying the mRNA *in situ* data. In transverse sections of adult mouse spinal cord, the *vrf* probes gave a neuronal staining pattern over the gray matter (fig. 2C). Counterstaining with toluidine (fig. 2D) showed that motoneurons in the ventral horn (fig. 2C and D) and interneurons (fig. 2C) in the deep part of the dorsal horn and around the central canal were to a large extent positive for *vrf* mRNA.

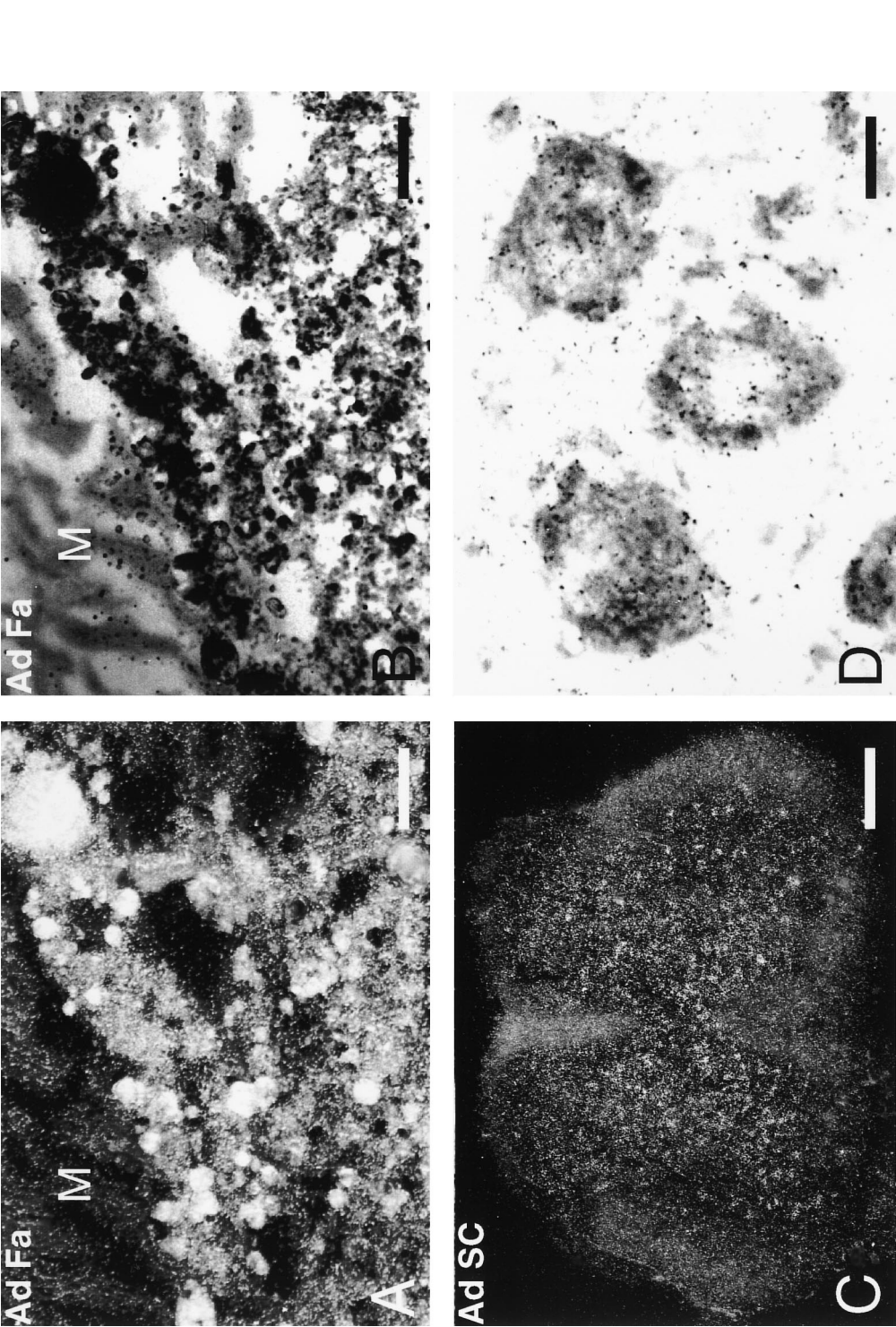


FIG. 2. Dark- (A and C) and bright-field (B and D) micrographs showing *vrf* mRNA expression in mouse adipose tissue (A–B) and spinal cord (C–D). A strong hybridization signal is present over fat (A), as shown by the strong labeling in Sudan black stained sections (B). A weak signal is present also in skeletal muscle (M in A–B). In the adult spinal cord (C) the *vrf* probes gave a neuronal staining pattern over the gray matter. Toluidine counterstaining showed that motoneurons in the ventral horn (D), interneurons in the deep part of the dorsal horn and around the central canal (not shown) were largely positive for *vrf* mRNA. Scale bars: 0.1 mm (A), 0.1 mm (B), 0.25 mm (C), 0.015 mm (D).

DISCUSSION

This paper describes the spatiotemporal expression pattern in mouse of a new member of the VEGF gene family, which we have designated VRF for VEGF Related Factor (Grimmond et al., submitted). The strong sequence homology between VEGF, PlGF and VRF reflect conservation of structural motifs of importance for peptide function (i.e. homo/heterodimerisation and heparin binding). The variable expression pattern of *vrf* during embryogenesis is consistent with the idea that murine *vrf* acts as a growth factor for certain tissues, such as the cerebral cortex, at a stage of rapid growth.

The *veg*f is expressed in a variety of developing (12, 13) and adult rodent tissues, such as brain, kidney, liver, lung, and spleen (14). This pattern has lead to the suggestion that *veg*f expression is regulated by steroid hormones (15). Mouse *vrf* appears to differ from VEGF in its expression pattern, although their expression partially overlaps as in heart. VEGF is overexpressed during tumor-associated angiogenesis (3), whereas we observed no overexpression of VRF in a panel of gliomas, breast carcinomas, and hypernephromas (Grimmond et al., submitted). VEGF and VRF thus appear to be regulated in different manners.

Several secretory and nonsecretory growth factors have been described as involved in angiogenesis (16), VEGF representing the most potent of them. The function of VEGF has often been connected to pathogenic processes such as inflammatory angiogenesis (17), tumor promoting angiogenesis (18), rheumatoid arthritis (19), diabetes related retinopathy (20) and myocardial ischaemia (21). Recently a potent inhibitor of angiogenesis in tumors was discovered, angiostatin, (22). Administration to young tumor bearing mice inhibited tumor growth, but did not effect normal growth and development until adulthood (Folkman, Nobel Forum lecture, Karolinska Institute). Several different regulatory pathways for vascularization should therefore be expected. We will investigate VRF as a candidate for controlling angiogenesis in normal tissue development.

ACKNOWLEDGMENTS

We thank Professor Tomas Hökfelt for expert advice. This work was supported by grants from the Swedish Cancer Foundation, the Swedish Medical Research Council, the Magn. Bergwall Fund, the Torsten och the Ragnar Söderberg Fund, the Åke Wiberg Fund, the Axel and Margret Ax:son Johnson Fund, the Fredrik and Ingrid Thuring Fund, AMRAD operations Pty. Ltd and the National Health and Medical Research Council of Australia.

REFERENCES

1. Keck, P. J., Hauser, S. D., Krivi, G., Sanzo, K., Warren, T., Feder, J., and Connolly, D. T. (1989) *Science* **246**, 1309–1312.
2. Leung, D. W., Cachianes, G., Kuang, W. J., Goeddel, D. V., and Ferrara, N. (1989) *Science* **246**, 1306–1309.
3. Senger, D. R., Van de Water, L., Brown, L. F., Nagy, J. A., Yeo, K. T., Yeo, T. K., Berse, B., Jackman, R. W., Dvorak, A. M., and Dvorak, H. F. (1993) *Cancer Metast. Rev.* **12**, 303–324.
4. Larsson, C., Weber, G., Kvanta, E., Lewis, C., Janson, M., Jones, C., Glaser, T., Evans, G., and Nordenskjöld, M. (1992) *Hum. Genet.* **89**, 187–193.
5. Weber, G., Friedman, E., Grimmond, S., Hayward, N., Phelan, C., Skogseid, B., Gobl, A., Carson, E., Sandelin, K., Teh, B. T., Zedenius, J., Oberg, K., Shepherd, J., Nordenskjöld, M., and Larsson, C. (1994) *Hum. Mol. Genet.* **3**, 1775–1781.
6. Lagercrantz, J., Larsson, C., Grimmond, S., Skogseid, B., Gobl, A., Friedman, E., Carson, E., Phelan, C., Öberg, K., Nordenskjöld, M., Hayward, N. K., and Weber, G. (1995) *J. Intern. Med.* **238**, 245–248.
7. Lagercrantz, J., Carson, E., Larsson, C., Nordenskjöld, M., Weber, G. Genomics, in press.
8. Houck, K. A., Ferrara, N., Winer, J., Cachianes, G., Li, G., and Leung, D. W. (1991) *Mol. Endocrinol.* **5**, 1806–1814.
9. Jacobsson, A., Muhleisen, M., Cannon, B., and Nedergaard, J. (1994) *Am. J. Physiol.* **267**, R999–R1007.
10. Houstek, J., Andersson, U., Tvrdik, P., Nedergaard, J., and Cannon, B. (1995) *J. Biol. Chem.* **270**, 7689–7694.
11. Dagerlind, A., Friberg, K., Bean, A. J., and Hökfelt, T. (1992) *Histochemistry* **98**, 39–49.
12. Breier, G., Albrecht, U., Sterrer, S., and Risau, W. (1992) *Development* **114**, 521–532.
13. Jakeman, L. B., Armanini, M., Phillips, H. S., and Ferrara, N. (1993) *Endocrinology* **133**, 848–859.
14. Monacci, W. T., Merrill, M. J., and Oldfield, E. H. (1993) *Am. J. Physiol.* **264**, C995–1002.
15. Shweiki, D., Itin, A., Neufeld, G., Gitay-Goren, H., and Keshet, E. (1993) *J. Clin. Invest.* **91**, 2235–2243.

16. Folkman, J. (1995) *Nat. Med.* **1**, 27–31.
17. Sunderkotter, C., Steinbrink, K., Goebeler, M., Bhardwaj, R., and Sorg, C. (1994) *J. Leukoc. Biol.* **55**, 410–422.
18. Christofori, G., Naik, P., and Hanahan, D. (1994) *Nature* **369**, 414–418.
19. Koch, A. E., Harlow, L. A., Haines, G. K., Amento, E. P., Unemori, E. N., Wong, W. L., Pope, R. M., and Ferrara, N. (1994) *J. Immunol.* **152**, 4149–4156.
20. Aiello, L. P., Avery, R. L., Arrigg, P. G., Keyt, B. A., Jampel, H. D., Shah, S. T., Pasquale, L. R., Thieme, H., Iwamoto, M. A., Park, J. E., Nguyen, H. V., Aiello, L. M., Ferrara, N., and King, G. L. (1994) *N. Engl. J. Med.* **331**, 1480–1487.
21. Banai, S., Shweiki, D., Pinson, A., Chandra, M., Lazarovici, G., and Keshet, E. (1994) *Cardiovasc. Res.* **28**, 1176–1179.
22. O'Reilly, M. S., Holmgren, L., Shing, Y., Chen, C., Rosenthal, R. A., Moses, M., Lane, W. S., Cao, Y., Sage, E. H., and Folkman, J. (1994) *Cell* **79**, 315–328.